

# Halocarbon Emissions from the United States and Mexico and Their Global Warming Potential

DYLAN B. MILLET,<sup>\*,†</sup> ELLIOT L. ATLAS,<sup>‡</sup>  
DONALD R. BLAKE,<sup>§</sup> NICOLA J. BLAKE,<sup>§</sup>  
GLENN S. DISKIN,<sup>||</sup> JOHN S. HOLLOWAY,<sup>⊥</sup>  
RYNDA C. HUDMAN,<sup>#</sup>  
SIMONE MEINARDI,<sup>§</sup>  
THOMAS B. RYERSON,<sup>⊥</sup> AND  
GLEN W. SACHSE<sup>||</sup>

University of Minnesota, St. Paul, Minnesota 55108,  
University of Miami, Miami, Florida 33149, University of  
California, Irvine, California 92697, NASA Langley Research  
Center, Hampton, Virginia 23681, NOAA CSD, Boulder,  
Colorado 80305, and University of California,  
Berkeley, California 94720

Received July 31, 2008. Revised manuscript received  
November 12, 2008. Accepted December 11, 2008.

We use recent aircraft measurements of a comprehensive suite of anthropogenic halocarbons, carbon monoxide (CO), and related tracers to place new constraints on North American halocarbon emissions and quantify their global warming potential. Using a chemical transport model (GEOS-Chem) we find that the ensemble of observations are consistent with our prior best estimate of the U.S. anthropogenic CO source, but suggest a 30% underestimate of Mexican emissions. We develop an optimized CO emission inventory on this basis and quantify halocarbon emissions from their measured enhancements relative to CO. Emissions continue for many compounds restricted under the Montreal Protocol, and we show that halocarbons make up an important fraction of the total greenhouse gas source for both countries: our best estimate is 9% (uncertainty range 6–12%) and 32% (21–52%) of equivalent CO<sub>2</sub> emissions for the U.S. and Mexico, respectively, on a 20 year time scale. Performance of bottom-up emission inventories is variable, with underestimates for some compounds and overestimates for others. Ongoing methylchloroform emissions are significant in the U.S. (2.8 Gg/y in 2004–2006), in contrast to bottom-up estimates (<0.05 Gg), with implications for tropospheric OH calculations. Mexican methylchloroform emissions are minor.

## Introduction

Anthropogenic halocarbons are potent greenhouse gases and deplete stratospheric ozone (1, 2). Methylchloroform (MCF, CH<sub>3</sub>CCl<sub>3</sub>) is also important as a widely used proxy for the hydroxyl radical (OH) (3–6), which defines the atmospheric lifetime of most greenhouse gases and other pollutants. Bottom-up source estimates (e.g., ref 7) for these compounds

rely largely on government and industry reports and have inherent uncertainties. Here we present new top-down constraints on halocarbon emissions from the United States and Mexico based on recent aircraft measurements, quantify the direct radiative forcing contribution of these emissions relative to those of other greenhouse gases, and assess the implications of ongoing MCF emissions for global OH estimates.

Under the Montreal Protocol and its subsequent amendments (8), production and consumption of chlorofluorocarbons (CFCs), halons, carbon tetrachloride (CCl<sub>4</sub>), and MCF were banned in developed countries as of 1996 (1994 for halons), with some limited critical-use exemptions. These compounds are also subject to a production phase-out for developing countries, culminating in a 2010 ban (2015 for MCF). Consumption and production of the transitional hydrochlorofluorocarbons (HCFCs) were frozen in 1996 and 2004, respectively, for developed countries, with a 100% phase-out mandated by 2030. For developing countries, HCFC consumption and production will be frozen in 2013, followed by sequential reductions culminating in a 100% phase-out by 2030 (9).

As a result of these measures, worldwide fluorocarbon production, weighted by global warming potential (GWP), has fallen substantially since its peak in 1988 according to industry and government reports (10, 11). However, reported production and sales figures are not necessarily accurate emission proxies in the Montreal Protocol era, as they do not account for stockpiling, recycling, or possible illicit production. In many cases, some postban emissions may be expected due to chemical banks in existing applications or in landfills.

Here, we apply recent aircraft measurements over the United States and Mexico to develop a new and robust understanding of North American halocarbon emissions and their atmospheric effects. The INTEX-A + ITCT-2K4 (collectively ICARTT), TEXAQS-II, and MILAGRO aircraft campaigns featured extensive boundary layer coverage over the U.S. and Mexico during 2004 and 2006. We use these data to derive halocarbon source fluxes on the basis of their relationship to carbon monoxide (CO) and other tracers.

## Materials and Methods

**Measurements.** Over the U.S., we use data from the NASA DC-8 aircraft during INTEX-A and the NOAA WP-3 aircraft during ITCT-2K4 and TEXAQS-II. INTEX-A and ITCT-2K4 took place during Jul-Aug 2004 as part of ICARTT (12, 13); INTEX-A was a broad-scale study extending across North America, whereas ITCT-2K4 was mainly in the U.S. Northeast and focused more on sampling urban plumes. TEXAQS-II took place over southern Texas during September–October 2006. Over Mexico, we use data from the NASA DC-8 and NSF C-130 aircraft during MILAGRO (March 2006). Supporting Information Figure S1 shows the flight-tracks for the above campaigns. For some compounds we compare the MILAGRO aircraft halocarbon:CO enhancement ratios (ERs) with data from the T0 (99.15°W, 19.49°N) and T1 (98.98°W, 19.70°N) ground sites in and downwind of Mexico City.

Halocarbons were measured by whole air sampling, with canisters shipped to the home laboratory postflight for analysis. Measurements were made by the UCI group for INTEX-A and MILAGRO, and by the Miami group for ITCT-2K4 and TEXAQS-II. Airborne CO measurements were made in situ on the aircraft, and by whole air canister sampling at the T0 and T1 ground sites. See the Supporting Information for details on the above measurements. Other in situ measurements used here to screen fresh biomass burning

\* Corresponding author email: dbm@umn.edu.

† University of Minnesota.

‡ University of Miami.

§ University of California, Irvine.

|| NASA Langley Research Center.

⊥ NOAA CSD.

# University of California, Berkeley.

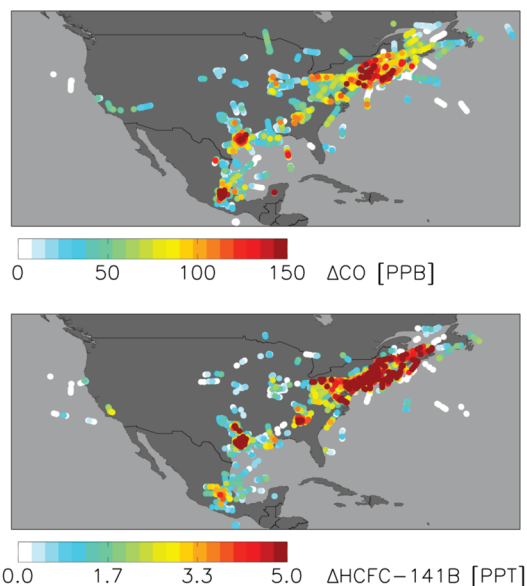


**FIGURE 1. CO (top) and HCFC-141B (bottom) enhancements measured in the boundary layer (<2 km) during the ICARTT, MILAGRO, and TEXAQS-II aircraft campaigns.**

and pollution plumes ( $\text{NO}$ ,  $\text{NO}_2$ ,  $\text{NO}_y$ ,  $\text{CH}_3\text{CN}$ ,  $\text{HCN}$ ) are described in detail elsewhere (14–21). For comparison with canister data, in situ measurements have been averaged over the canister fill times (or for some measurements the value for the corresponding minute has been used).

Figure 1 shows boundary layer (<2 km radar altitude) CO and HCFC-141B enhancements measured over North America. We calculate boundary layer pollution enhancements  $\Delta X$  for each compound X by subtracting background levels (derived for each campaign by interpolating the 0.1 concentration quantiles in  $10^\circ$  latitude bins) from the observed concentrations. Biomass burning plumes (diagnosed by  $\text{CH}_3\text{CN} > 225$  ppt or  $\text{HCN} > 425$  ppt) and statistical outliers (>0.98 quantile) are removed prior to calculating background levels and enhancements. The TEXAQS-II data are strongly influenced by near-field halocarbon emissions from the large petrochemical complex in the Houston Ship Channel; we apply in this case a more stringent statistical filter (excluding data >0.80 quantile) to ensure a regionally representative signal.

**CO Simulation and Comparison to Observations.** We use the GEOS-Chem (<http://www.as.harvard.edu/ctm/geos/>, see the Supporting Information) chemical transport model to evaluate and optimize current CO emission estimates on the basis of atmospheric observations, in order to then derive halocarbon emissions from measured halocarbon:CO ERs.

The GEOS-Chem CO simulation is as described by Duncan et al. (22), with the following modifications. Emissions of biogenic hydrocarbons are as described by Millet et al. (23). Biomass burning emissions are from the GFEDv2 inventory (24), though in all comparisons that follow we filter out fire plumes. The U.S. anthropogenic CO source is based on the work of Hudman et al. (25), who showed that emissions are 60% lower than specified in the U.S. EPA inventory for 1999. That work is supported by other studies showing that the EPA anthropogenic CO source is too high (25–28). As we show later, the corresponding GEOS-Chem simulation is consistent with the INTEX-A, ITCT-2K4, and TEXAQS-II aircraft observations. The resulting U.S. anthropogenic CO source is 34 Tg/y. For more details on the U.S. anthropogenic CO inventory used here, see Hudman et al. (25).

Anthropogenic CO emissions in northern Mexico are from BRAVO (29), a bottom-up emission inventory for CO and other pollutants covering the 10 northern Mexican states

plus Mexico City. Over southern Mexico, anthropogenic CO emissions are as described by Duncan et al. (22). Both of these inventories have been described in detail elsewhere (22, 29–31), and we refer the reader to those publications for more information. Here, we evaluate these inventories using the MILAGRO aircraft measurements.

Initial GEOS-Chem simulations revealed a low bias over Mexico, with a reduced major axis (RMA) (32) slope of 0.87 relative to the MILAGRO observations. We attribute this discrepancy to an underestimate of Mexican anthropogenic CO emissions as other possibilities do not appear tenable. MILAGRO took place in March, so that biogenic VOC oxidation is not likely a major CO source. Biomass burning plumes have been screened from the data, and Yokelson et al. (33) estimated that pyrogenic CO was in any case only 15% of the urban source during MILAGRO. For comparison, in our base-case GEOS-Chem simulation, the Mexican fire contribution to CO mixing ratios along the MILAGRO flight-tracks is 19% (median value) of that from Mexican fossil fuel. The main sink for near-surface CO is boundary layer ventilation (chemical oxidation is slow in comparison), and previous work with GEOS-Chem argues against a persistent model bias in this process (23, 25, 34).

We find that increasing the Mexican anthropogenic CO source by 30% (to 12 Tg/y) gives a model:measurement slope which is statistically indistinguishable from one ( $0.92 \pm 0.12$ , Supporting Information Figure S2), and we adopt this as best estimate for deriving Mexican halocarbon emissions from halocarbon:CO ERs. Here and below, quoted uncertainties reflect 95% confidence intervals (CIs) determined by bootstrap resampling (subsampling with replacement, 10 000 trials,  $n$  = sample size). Two independent constraints provide further support for our optimized Mexican CO source. First, the 30% adjustment yields annual CO emissions for the Mexico City grid cell which agree well with the latest emission inventory from the Mexico City Secretary of the Environment (35) (both 2.0 Tg/y for 2006). Second, the median ratio of fire:urban CO (for Mexican sources) along the MILAGRO flight-tracks in the model is then 16%, in agreement with the Yokelson et al. findings.

Supporting Information Figure S2 shows simulated vs observed boundary layer CO concentrations during ICARTT, TEXAQS-II, and MILAGRO. Biomass burning and fresh pollution plumes ( $\text{NO}_2 > 4$  ppb or  $\text{NO}_x:\text{NO}_y > 0.4$ ) have been removed since they are not captured at the  $2 \times 2.5^\circ$  model resolution. In all cases the RMA slopes are near-unity ( $\pm 0.08$ ) indicating that we can use the CO source terms above to derive robust top-down U.S. and Mexican halocarbon emission rates. The TEXAQS-II comparison is the only case with a statistically significant offset ( $25 \pm 5$  ppb). This reflects a bias in the modeled CO background for this location and season, but not in the regional CO emissions (these are validated by the slope of  $1.03 \pm 0.05$ ).

**Quantifying Halocarbon Sources and Uncertainty Estimates.** Supporting Information Figures S3 and S4 show boundary layer  $\Delta X:\Delta\text{CO}$  correlations for each halocarbon X over the U.S. and Mexico, with ERs and correlation coefficients given in Supporting Information Tables S1 and S2. As above, quoted uncertainties reflect 95% CIs (bootstrap method). Biomass burning plumes and statistical outliers have been removed as above. While U.S. CO sources during summer include a significant contribution from the oxidation of biogenic hydrocarbons (25), the halocarbon:CO ERs are determined by the ratio of the anthropogenic sources: biogenic CO sources will generally degrade the correlation coefficients but not affect the slopes.

We derive a best estimate of the average national ER for each halocarbon from the mean of the individual aircraft data sets. See Supporting Information Tables S1 and S2. ERs not distinguishable from 0 with 95% confidence are assumed

**TABLE 1. Halocarbon Emissions from the U.S. and Mexico and Their Global Warming Potential<sup>a</sup>**

|   | U.S. emissions (Gg/y) | U.S. GWP (TgCO <sub>2</sub> equiv) |                  | Mexico emissions (Gg/y) | Mexico GWP (TgCO <sub>2</sub> equiv) |                  |
|---|-----------------------|------------------------------------|------------------|-------------------------|--------------------------------------|------------------|
|   |                       | 20 Year                            | 100 Year         |                         | 20 Year                              | 100 Year         |
| CH <sub>2</sub> Cl <sub>2</sub>               | 24 (16–32)            | 0.8 (0.5–1.0)                      | 0.21 (0.14–0.28) | 6.8 (3.0–11)            | 0.2 (0.1–0.3)                        | 0.06 (0.03–0.09) |
| CHCl <sub>3</sub>                             | 13 (10–17)            | 1.3 (1.0–1.7)                      | 0.40 (0.29–0.51) | 2.1 (1.2–3.9)           | 0.2 (0.1–0.4)                        | 0.06 (0.04–0.12) |
| CCl <sub>4</sub>                              | ND                    |                                    |                  | ND                      |                                      |                  |
| CH <sub>3</sub> CCl <sub>3</sub> <sup>b</sup> | 2.8 (2.0–3.5)         | 1.4 (1.0–1.8)                      | 0.40 (0.29–0.51) | 0.1 (0.06–0.13)         | 0.05 (0.03–0.07)                     | 0.01 (0.01–0.02) |
| CH <sub>2</sub> ClCH <sub>2</sub> Cl          | 7.2 (1.5–16)          |                                    |                  | 13 (2.8–45)             |                                      |                  |
| C <sub>2</sub> HCl <sub>3</sub>               | 7.6 (4.8–10)          |                                    |                  | 0.9 (0.5–1.4)           |                                      |                  |
| C <sub>2</sub> Cl <sub>4</sub>                | 26 (15–40)            |                                    |                  | 8.7 (2.6–17)            |                                      |                  |
| HCFC-21                                       | 0.2 (0.1–0.3)         | 0.11 (0.05–0.16)                   | 0.03 (0.01–0.05) | NM                      | NM                                   | NM               |
| HCFC-22                                       | 46 (21–69)            | 239 (109–355)                      | 84 (38–124)      | 7.5 (4.4–12)            | 39 (23–60)                           | 14 (7.9–21)      |
| HCFC-123                                      | 0.4 (0.2–0.5)         | 0.10 (0.07–0.14)                   | 0.03 (0.02–0.04) | NM                      | NM                                   | NM               |
| HCFC-124                                      | 1.0 (0.4–1.6)         | 2.1 (0.9–3.4)                      | 0.6 (0.3–1.0)    | NM                      | NM                                   | NM               |
| HCFC-141B                                     | 4.5 (2.2–6.8)         | 10 (4.9–15)                        | 3.3 (1.6–4.9)    | 1.6 (1.0–2.4)           | 3.7 (2.2–5.3)                        | 1.2 (0.7–1.7)    |
| HCFC-142B                                     | 5.2 (2.4–9.2)         | 28 (13–50)                         | 12 (5.6–21)      | 0.9 (0.4–1.4)           | 4.9 (2.2–7.8)                        | 2.0 (0.9–3.3)    |
| HFC-134A                                      | 27 (12–39)            | 102 (46–148)                       | 38 (17–55)       | 2.9 (1.7–4.3)           | 11 (6.5–17)                          | 4.1 (2.4–6.2)    |
| HFC-152A                                      | 7.6 (5.7–9.7)         | 3.3 (2.5–4.2)                      | 0.9 (0.7–1.2)    | NM                      | NM                                   | NM               |
| H-1211  | 0.6 (0.3–0.8)         | 2.7 (1.5–3.8)                      | 1.1 (0.6–1.5)    | 0.1 (0–0.3)             | 0.6 (0–1.5)                          | 0.2 (0–0.6)      |
| H-1301  | ND                    |                                    |                  | ND                      |                                      |                  |
| H-2402  | ND                    |                                    |                  | ND                      |                                      |                  |
| CFC-11  | 11 (7.0–14)           | 71 (47–95)                         | 50 (33–67)       | 5.1 (2.7–8.8)           | 34 (18–59)                           | 24 (13–42)       |
| CFC-12  | 8.8 (0–16)            | 97 (0–177)                         | 96 (0–175)       | 3.5 (0–11)              | 39 (0–118)                           | 39 (0–117)       |
| CFC-113                                       | ND                    |                                    |                  | ND                      |                                      |                  |
| CFC-114                                       | 0.2 (0–0.8)           | 1.9 (0–6.1)                        | 2.3 (0–7.6)      | 0.3 (0–0.7)             | 2.2 (0–6.0)                          | 2.7 (0–7.5)      |
| CFC-115                                       | 0.4 (0–0.9)           | 2.2 (0–4.9)                        | 3.1 (0–6.8)      | NM                      | NM                                   | NM               |
| <b>TOTAL:</b>                                 |                       | 563 (389–715)                      | 292 (182–385)    |                         | 135 (89–221)                         | 87 (46–168)      |

<sup>a</sup> Emissions calculated based on the mean  $\Delta X/\Delta CO$  slope from the aircraft missions. Emission and GWP uncertainties for each compound reflect the total range encompassed by the 95% CIs for the aircraft ERs, combined with the estimated uncertainty of the CO emissions and halocarbon seasonality. See text. Uncertainties for the total GWP are derived by propagating the individual errors in quadrature. ND: not detectable. NM: not measured. Data reflect a 2004–6 average for the U.S., and 2006 for Mexico. <sup>b</sup> Mexican CH<sub>3</sub>CCl<sub>3</sub> emissions calculated based on measurements at the T0 ground station during MILAGRO.

to be “undetectable” for that data set and included in the average as zero. We set the overall ER to zero (undetectable emissions) in cases where none of the individual ERs are statistically nonzero or if the correlation coefficients are all <0.3. Since INTEX-A and ITCT-2K4 took place in 2004, while TEXAQS-II and MILAGRO took place in 2006, the emission estimates that follow reflect 2004–2006 for the U.S., and 2006 for Mexico.

Supporting Information Tables S1 and S2 show that, for a few compounds, the measured ERs vary significantly between data sets. We attribute such cases to regional emission ratio variability, not instrumental offsets. The UCI and Miami groups routinely cross-compare calibration standards, and airborne wingtip-to-wingtip double-blind intercomparisons during the campaigns showed good agreement. Expected measurement discrepancies are a few percent or less. We use the total range encompassed by all 95% CIs for the individual aircraft data sets as a conservative error estimate for each national best-estimate ER (e.g., the uncertainty range includes 0 if enhancements were undetectable for any individual data set).

The national ERs are then multiplied by the corresponding anthropogenic CO flux to obtain halocarbon emission rates for each country, adjusting for the seasonality of emissions. We account for emission seasonality using 3 years of halocarbon and CO measurements in the U.S. Northeast (36) (see the Supporting Information). The resulting U.S. and Mexican emissions for each compound are given in Table 1.

Uncertainty ranges for halocarbon emissions are calculated by propagating (in quadrature) the uncertainties associated with the ER, national CO flux, and seasonality factor. We assume an uncertainty of 20% for the U.S. anthropogenic CO source and 30% for Mexico. The Barnes et al. (36) seasonal  $\Delta X:\Delta CO$  adjustment factors for any one year are generally within 15% of their observed 3 year means, and we use that as an estimate of the seasonality uncertainty.

The accuracy of national emission estimates depends on the representativeness of the measured ERs. This is the most extensive data set that has been used for such an analysis, so that representation error should be less than in earlier work.

### North American Halocarbon Emission Rates

**MCF.** MCF (atmospheric lifetime 5–6 years) is widely used to constrain global OH abundance, and to infer its interannual variability (3–6, 37, 38). Interannual OH trends derived from MCF are highly sensitive to the assumed emission rates, and the extent of ongoing industrialized emissions since the 1996 ban is disputed (39–42). In the U.S., bottom-up calculations by the EPA imply annual emissions <0.05 Gg since 1997 (43). Millet and Goldstein (41) presented evidence of significant ongoing U.S. emissions (3.7 Gg/y in 2002) in the postban era, based on measurements in two cities, a finding supported by subsequent aircraft measurements during COBRA-NA (39). However, the accuracy of both findings hinges on that of the bottom-up CO emissions used to calculate the fluxes. Li et al. (40) estimated a 50% lower U.S. MCF source, but using data from a single site (on the remote Northern California coast) which is ill-suited for assessing national emissions.

Here, we obtain statistically consistent  $\Delta MCF:\Delta CO$  ERs (17, 18, and 17 ppt/ppm) from all three aircraft over the geographically extensive ITCT-2K4/INTEX-A/TEXAQS-II domain. Combining the average of these with the independently constrained U.S. CO source, we derive U.S. MCF emissions of 2.8 (uncertainty range 2.0–3.5) Gg/y in 2004–2006. This is more than 50 times the EPA estimate and confirms the earlier Millet and Goldstein (41) and Hurst et al. (39) findings, given the estimated decay rate of residual MCF emissions (e-folding time 3.1 y) (41). U.S. emissions thus continue to be a significant source of atmospheric MCF despite the 1996 ban. As we discuss later, these emissions need to be accounted for when inferring interannual changes in OH.



Airborne MCF measurements are not available for MILAGRO, and we instead use data from the T0 ground site in Mexico City to estimate Mexican emissions. The measured ER (1.7 ppt/ppm) is a factor of 10 lower than the U.S. value (emissions are undetectable at the T1 site). Our calculated Mexican emissions are minor: 0.1 (0.06–0.13) Gg/y in 2006, which is consistent with data reported to the UNEP (zero consumption since 2002) (11). However, this estimate carries the caveat that ground-based measurements at T0 may not perfectly represent the overall Mexican source.

**CFCs.** CFC-11 and CFC-12 have statistically significant correlations with CO over the U.S., and the corresponding best-estimate emissions are 11 (7–14) and 8.8 (0–16) Gg/y. CFC-114 and 115 emissions are barely detectable (only detected during ITCT-2K4), and the measured ERs imply U.S. emissions of 0.2 (0–0.8) and 0.4 (0–0.9) Gg/y (all of the above for 2004–2006). Our results for CFC-11 and CFC-12 are consistent (within uncertainty) with estimates by Hurst et al. for 2003 ( $7 \pm 3$  Gg/y and  $14 \pm 4$  Gg/y) (39) and the EPA for 2004 (9 Gg/y and 13 Gg/y) (43). However, U.S. CFC-115 emissions appear to be lower than the current estimate of 2.0 Gg/y in 2004 (43).

Based on the MILAGRO data set we estimate Mexican CFC-11 and 12 emissions of 5.1 (2.7–8.8) and 3.5 (0–11) Gg/y in 2006. Emissions for both are near detection limit: the largest enhancements are only 2–3% above background (vs a 1% measurement precision), and CFC-12 emissions were only detected from the DC-8. Since CFC-11 and 12 account for a large fraction of the total halocarbon GWP for Mexico, we used data from the T0 and T1 ground stations to further evaluate the Mexican source of these compounds (see the Supporting Information). Emissions are clearly detectable at the ground sites, though the ERs are lower than the aircraft values.

Including CFC-114 emissions of 0.3 (0–0.7) Gg/y, our best estimate of total Mexican CFC emissions is 3–5 times higher than reported Mexican consumption for any year since 1999 (11). However, the associated uncertainty range is large (2.7–21 Tg/y in 2006) since measured enhancements are such a small fraction of background levels. CFC-113 enhancements were not detectable during any of the aircraft campaigns, showing that U.S. and Mexican emissions of this compound have effectively ceased.

**Halons.** U.S. halon-1211 emissions continue despite the 1994 ban under the Montreal Protocol, with a total source of 0.6 (0.3–0.8) Gg/y in 2004–2006, statistically consistent with earlier estimates for 2003–2004 (39, 43). The U.S. EPA estimates 2004 H-1301 emissions at 1.5 Gg (43), but in fact we find that emissions are undetectable for H-1301 and for H-2402 (the EPA does not provide an estimate for H-2402). Mexican H-1211 emissions were detected from the C-130 aircraft only, yielding a national flux estimate of 0.1 (0–0.3) Gg/y in 2006. H-1301 and H-2402 emissions were not detectable from Mexico.

**HCFCs.** U.S. HCFC-22 emissions are substantial (best estimate 46 Gg/y in 2004–2006), and as we shall see this compound is the single largest contributor to the U.S. halocarbon GWP. Measured ERs relative to CO differ by more than a factor of 2 (Supporting Information Table S1), and the uncertainty range based on the combined 95% CIs for the three aircraft campaigns is 21–69 Gg/y. Our best estimate for the U.S. source is 45% lower than the EPA's bottom-up estimate (83 Gg in 2004) (43).

Based on the combined U.S. data sets, HCFC-141B and 142B emissions were 4.5 (2.2–6.8) and 5.2 (2.4–9.2) Gg/y in 2004–2006. Our best estimates are 15 and 60% higher than the 2004 EPA values for the two compounds (43), though in both cases the EPA estimates fall within our uncertainty range. We find that U.S. emissions of other HCFCs are minor in comparison to the above compounds, with best estimates of

0.2 (0.1–0.3), 0.4 (0.2–0.5), and 1.0 (0.4–1.6) Gg/y for HCFC-21, 123, and 124 (2004–6). The EPA provides estimates for HCFC-123 and 124 only (0.8 and 1.5 Gg/y in 2004) (43).

The major HCFCs were measured during the airborne portion of MILAGRO, and on the basis of that data set we derive best-estimate emissions of 7.5 (4.4–12), 1.6 (1.0–2.4), and 0.9 (0.4–1.4) Gg in 2006 for HCFC-22, HCFC-141B, and HCFC-142B (Table 1).

**HFCs.** HFCs do not contain chlorine or bromine and so do not deplete stratospheric ozone, but they are effective greenhouse gases, with GWPs up to  $15\,000 \times$  that of CO<sub>2</sub> (44). HFC-134a is the predominant HFC emitted from the U.S.: our best estimate is 27 Gg/y in 2004–2006, with an uncertainty range of 12–39 Gg/y. This is significantly lower than the EPA bottom-up estimate (57 Gg in 2004) (43). HFC-152A was measured during TEXAQS-II but not ICARTT, and we estimate U.S. emissions of 7.6 (5.7–9.7) Gg/y in 2006 using that data set. HFC-134a was the only HFC measured over Mexico, and our best estimate is 2.9 (1.7–4.3) Gg emitted in 2006.

**Other Halocarbons.** Table 1 gives best estimates and uncertainty ranges for U.S. and Mexican emissions of other anthropogenic halocarbons. In the case of C<sub>2</sub>HCl<sub>3</sub> our derived flux may be a conservative estimate due to non-negligible photochemical loss relative to CO prior to sampling (atmospheric lifetime 2.6 days at OH =  $2 \times 10^6$  molec/cm<sup>3</sup>). Other compounds considered have atmospheric lifetimes of weeks or longer with respect to oxidation by OH.

Our best estimate of the total U.S. CHCl<sub>3</sub> source (13 Gg/y in 2004–2006, uncertainty range 10–17 Gg/y) agrees well with work by Hurst et al. (39). We find that North American emissions of CCl<sub>4</sub> are undetectable. Performance of the EPA NEI 2002 (45) for these other halocarbons is variable. Emissions of CHCl<sub>3</sub> and CH<sub>2</sub>ClCH<sub>2</sub>Cl are strongly underestimated (factors of 2 and 18 using our best estimates), while those of CH<sub>2</sub>Cl<sub>2</sub> are too high (factor of 1.9). The NEI estimate for C<sub>2</sub>Cl<sub>4</sub> (32 Gg/y in 2002) is consistent with our findings. Over both Mexico and the U.S., ERs for CH<sub>2</sub>Cl<sub>2</sub>, C<sub>2</sub>Cl<sub>4</sub> and CH<sub>2</sub>ClCH<sub>2</sub>Cl vary quite widely, and the estimated emissions have a correspondingly large uncertainty range.

## Global Warming Potential of Current U.S. and Mexican Halocarbon Emissions

Figure 2 shows the weighted global warming potential (emission rate  $\times$  GWP 2, 44) of U.S. and Mexican halocarbon emissions on 20, 100, and 500 year time horizons, expressed as Tg of CO<sub>2</sub> equivalents. Uncertainty estimates for the total weighted halocarbon GWP for each country are calculated by propagating (in quadrature) those for the individual compounds. We find that on a 20 year time scale, current halocarbon emissions are the third largest component of the overall long-lived greenhouse gas source from both countries, after CO<sub>2</sub> and methane and before N<sub>2</sub>O. As above, our data reflect a 2004–2006 average for the U.S., and 2006 for Mexico.

We estimate total U.S. halocarbon emissions of 563 TgCO<sub>2</sub> Eq. on a 20-year time scale, with an uncertainty range of 389–715 TgCO<sub>2</sub> equiv. This is equal to 9% (6–12%), 30% (21–38%), and 170% (110–210%) of current U.S. CO<sub>2</sub>, methane, and N<sub>2</sub>O emissions, respectively (also on a 20 year time scale) (43). HCFC-22, CFC-12, HFC-134a, and CFC-11 are the main contributors, and will account for 90% of the total U.S. halocarbon radiative forcing over the next 20 years (Table 1).

In Mexico, we find that current halocarbon emissions are equivalent to 135 (89–221) TgCO<sub>2</sub> on a 20 year time scale. This value is sensitive to the estimates for CFC-11 and -12, whose emissions are near detection limit for the MILAGRO airborne data sets. If instead we average the T0 and T1 ERs for these compounds (see the Supporting Information), we

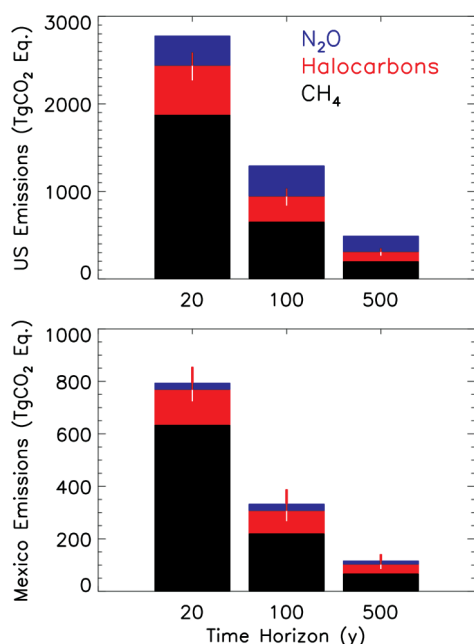


**FIGURE 2.** Global warming potential of current U.S. and Mexican emissions of non-CO<sub>2</sub> long-lived greenhouse gases expressed as teragrams of CO<sub>2</sub> equivalents, over 20, 100, and 500-year time horizons. Halocarbon emissions (in red) are those derived here, with the error-bars showing the estimated uncertainty as described in the text. Methane (black) and N<sub>2</sub>O (blue) emissions are based on published estimates (43, 46, 47). Data reflect a 2004–2006 average for the U.S., and 2006 for Mexico (Mexican CH<sub>4</sub> and N<sub>2</sub>O emissions are for 2005, the latest available year).

obtain an overall best estimate of 104 TgCO<sub>2</sub> equiv (20 year time scale), still within our uncertainty range. Halocarbons thus make up a large fraction of Mexico's greenhouse gas budget, equivalent to 32% (21–52%) of current CO<sub>2</sub> emissions, 21% (14–35%) of methane, and 540% (360–890%) of N<sub>2</sub>O over the next 20 years (46, 47).

As we see, the Montreal Protocol has been very effective at reducing global emissions of ozone-depleting substances, but ongoing halocarbon emissions in the U.S. and Mexico still make up an important fraction of their overall greenhouse gas source. Our results show that both countries (Mexico in particular) have an opportunity to make a sizable cut in their greenhouse gas footprint by targeting these halocarbons.

### U.S. MCF Emissions and Implications for OH Estimates

We find that U.S. MCF emissions were 2.8 (2.0–3.5) Gg/y in 2004–2006, versus an EPA estimate of <0.05 Gg/y (43). If the U.S. accounts for the same fraction (44% average over 1989–1995 (11)) of industrialized emissions as prior to the phase-out (other developed nations are subject to the same production and consumption restrictions under the Montreal Protocol), this would imply 6.4 Gg/y of global unreported emissions over this 2004–2006 time frame. Uncounted emissions of this magnitude would bias inferred interannual OH changes (5, 37, 38, 41). For example, 11 Gg of fugitive emissions globally was estimated to yield an OH bias of ~5% (41).

As pointed out by Prinn et al. (5), the extent of the effect depends on whether ongoing emissions reflect illegal imports from reporting Northern Hemisphere producers rather than a time lag between sales and emission or illicit production and use. A recent inversion study by Wang et al. (38), optimizing simultaneously for OH abundance and MCF emissions, implies that earlier (1988–1994) MCF emissions may be substantially lower than presently thought. An

underestimate of the time lag between MCF sales and emission thus appears likely. OH inversions need to include a priori errors that are sufficient to reflect the true uncertainty in global MCF source estimates.

### Acknowledgments

We thank T. Campos, R. Cohen, J. de Gouw, G. Huey, T. Karl, H. Singh, A. Weinheimer, and P. Wennberg for sharing their measurements, and D. Parrish for helpful discussion.

### Supporting Information Available

ΔX:ΔCO halocarbon ERs and 95% CIs are provided in Tables S1 and S2. Flight-tracks for the aircraft campaigns are shown in Figure S1, scatterplots of simulated versus observed boundary layer CO are shown in Figure S2, and halocarbon:CO correlation plots over the U.S. and Mexico are provided in Figures S3 and S4. Information on halocarbon and CO measurements, the GEOS-Chem model, halocarbon seasonal adjustment factors, and T0/T1 CFC enhancements is also provided. This material is available free of charge via the Internet at <http://pubs.acs.org>.

### Literature Cited

- Clerbaux, C.; Cunnold, D. M. Chapter 1: Long-Lived Compounds. In *Scientific Assessment of Ozone Depletion: 2006*, Global Ozone Research and Monitoring Project - Report No. 50; WMO: Geneva, 2006.
- Forster, P.; Ramaswamy, V. Changes in Atmospheric Constituents and in Radiative Forcing. In *Climate Change 2007: The Physical Science Basis*; Solomon, S., Qin, D., Manning, M., Chen, Z., Marquis, M., Averyt, K. B., Tignor, M., Miller, H. L., Eds.; Cambridge University Press: New York, 2007.
- Krol, M.; Lelieveld, J. Can the variability in tropospheric OH be deduced from measurements of 1,1,1-trichloroethane (methyl chloroform)? *J. Geophys. Res.* **2003**, *108*, 4125, doi: 10.1029/2002JD002423.
- Montzka, S. A.; Spivakovsky, C. M.; Butler, J. H.; Elkins, J. W.; Lock, L. T.; Mondeel, D. J. New observational constraints for atmospheric hydroxyl on global and hemispheric scales. *Science* **2000**, *288*, 500–503.
- Prinn, R. G.; Huang, J.; Weiss, R. F.; Cunnold, D. M.; Fraser, P. J.; Simmonds, P. G.; McCulloch, A.; Harth, C.; Reimann, S.; Salameh, P.; O'Doherty, S.; Wang, R. H. J.; Porter, L. W.; Miller, B. R.; Krummel, P. B. Evidence for variability of atmospheric hydroxyl radicals over the past quarter century. *Geophys. Res. Lett.* **2005**, *32*, L07809, doi:10.1029/2004GL022228.
- Spivakovsky, C. M.; Logan, J. A.; Montzka, S. A.; Balkanski, Y. J.; Foreman-Fowler, M.; Jones, D. B. A.; Horowitz, L. W.; Fusco, A. C.; Brenninkmeijer, C. A. M.; Prather, M. J.; Wofsy, S. C.; McElroy, M. B. Three-dimensional climatological distribution of tropospheric OH: Update and evaluation. *J. Geophys. Res.* **2000**, *105*, 8931–8980.
- Aucott, M. L.; McCulloch, A.; Graedel, T. E.; Kleiman, G.; Midgley, P.; Li, Y. F. Anthropogenic emissions of trichloromethane (chloroform, CHCl<sub>3</sub>) and chlorodifluoromethane (HCFC-22): Reactive Chlorine Emissions Inventory. *J. Geophys. Res.* **1999**, *104*, 8405–8415.
- UNEP. The Montreal Protocol on Substances that Deplete the Ozone Layer; United Nations Environment Programme: Nairobi, 2000.
- UNEP 2007 Montreal Adjustment on Production and Consumption of HCFCs. <http://ozone.unep.org/>.
- AFEAS Alternative Fluorocarbons Environmental Acceptability Study. <http://www.afeas.org>.
- UNEP. *Production and consumption of ozone depleting substances under the Montreal Protocol: 1986–2004*; United Nations Environment Programme: Nairobi, 2005.
- Fehsenfeld, F. C.; Ancellet, G.; Bates, T. S.; Goldstein, A. H.; Hardesty, R. M.; Honrath, R.; Law, K. S.; Lewis, A. C.; Leitch, R.; McKeen, S.; Meagher, J.; Parrish, D. D.; Pszenny, A. A. P.; Russell, P. B.; Schlager, H.; Seinfeld, J.; Talbot, R.; Zbinden, R. International Consortium for Atmospheric Research on Transport and Transformation (ICARTT): North America to Europe—Overview of the 2004 summer field study. *J. Geophys. Res.* **2006**, *111*, D23S01, doi: 10.1029/2006JD007829.

- (13) Singh, H. B.; Brune, W. H.; Crawford, J. H.; Jacob, D. J.; Russell, P. B. Overview of the summer 2004 intercontinental chemical transport experiment - North America (INTEX-A). *J. Geophys. Res.* **2006**, *111*, D24S01, doi: 10.1029/2006JD007905.
- (14) Crounse, J. D.; McKinney, K. A.; Kwan, A. J.; Wennberg, P. O. Measurement of gas-phase hydroperoxides by chemical ionization mass spectrometry. *Anal. Chem.* **2006**, *78*, 6726–6732.
- (15) Day, D. A.; Wooldridge, P. J.; Dillon, M. B.; Thornton, J. A.; Cohen, R. C. A thermal dissociation laser-induced fluorescence instrument for in situ detection of NO<sub>2</sub>, peroxy nitrates, alkyl nitrates, and HNO<sub>3</sub>. *J. Geophys. Res.* **2002**, *107*, 4046, doi: 10.1029/2001JD000779.
- (16) de Gouw, J. A.; Warneke, C.; Parrish, D. D.; Holloway, J. S.; Trainer, M.; Fehsenfeld, F. C. Emission sources and ocean uptake of acetonitrile (CH<sub>3</sub>CN) in the atmosphere. *J. Geophys. Res.* **2003**, *108*, 4329, doi: 10.1029/2002JD002897.
- (17) Karl, T.; Apel, E.; Hodzic, A.; Riemer, D. D.; Blake, D. R.; Wiedinmyer, C. Emissions of volatile organic compounds inferred from airborne flux measurements over a megacity. *Atmos. Chem. Phys.* **2009**, *9*, 271–285.
- (18) Ryerson, T. B.; Williams, E. J.; Fehsenfeld, F. C. An efficient photolysis system for fast-response NO<sub>2</sub> measurements. *J. Geophys. Res.* **2000**, *105*, 26447–26461.
- (19) Singh, H. B.; Salas, L.; Herlth, D.; Kolyer, R.; Czech, E.; Viezee, W.; Li, Q.; Jacob, D. J.; Blake, D.; Sachse, G.; Harward, C. N.; Fuelberg, H.; Kiley, C. M.; Zhao, Y.; Kondo, Y. In situ measurements of HCN and CH<sub>3</sub>CN over the Pacific Ocean: Sources, sinks, and budgets. *J. Geophys. Res.* **2003**, *108*, 8795, doi: 10.1029/2002JD003006.
- (20) Sjostedt, S. J.; Huey, L. G.; Tanner, D. J.; Peischl, J.; Chen, G.; Dibb, J. E.; Lefter, B.; Hutterli, M. A.; Beyersdorf, A. J.; Blake, N. J.; Blake, D. R.; Sueper, D.; Ryerson, T.; Burkhardt, J.; Stohl, A. Observations of hydroxyl and the sum of peroxy radicals at Summit, Greenland during summer 2003. *Atmos. Environ.* **2007**, *41*, 5122–5137.
- (21) Weinheimer, A. J.; Walega, J. G.; Ridley, B. A.; Sachse, G. W.; Anderson, B. E.; Collins, J. E. Stratospheric NO<sub>y</sub> measurements on the NASA DC-8 during AASE-II. *J. Geophys. Res. Lett.* **1993**, *20*, 2563–2566.
- (22) Duncan, B. N.; Logan, J. A.; Bey, I.; Megretskaia, I. A.; Yantosca, R. M.; Novelli, P. C.; Jones, N. B.; Rinsland, C. P. Global budget of CO, 1988–1997: Source estimates and validation with a global model. *J. Geophys. Res.* **2007**, *112*, D22301, doi: 10.1029/2007JD008459.
- (23) Millet, D. B.; Jacob, D. J.; Turquety, S.; Hudman, R. C.; Wu, S.; Fried, A.; Walega, J.; Heikes, B. G.; Blake, D. R.; Singh, H. B.; Anderson, B. E.; Clarke, A. D. Formaldehyde distribution over North America: Implications for satellite retrievals of formaldehyde columns and isoprene emission. *J. Geophys. Res.* **2006**, *111*, D24S02, doi: 10.1029/2005JD006853.
- (24) Randerson, J. T.; van der Werf, G. R.; Giglio, L.; Collatz, G. J.; Kasibhatla, P. S. *Global Fire Emissions Database Version 2 (GFEDv2)*; Oak Ridge National Laboratory Distributed Active Archive Center: Oak Ridge TN, 2006; idoi: 10.3334/ORNLDAA/834.
- (25) Hudman, R. C.; Murray, L. T.; Jacob, D. J.; Millet, D. B.; Turquety, S.; Wu, S.; Blake, D. R.; Goldstein, A. H.; Holloway, J.; Sachse, G. W. Biogenic vs. anthropogenic sources of CO over the United States. *Geophys. Res. Lett.* **2008**, *35*, L04801, doi: 10.1029/2007GL032393.
- (26) Millet, D. B.; Goldstein, A. H.; Holzinger, R.; Williams, B. J.; Allan, J. D.; Jimenez, J. L.; Worsnop, D. R.; Roberts, J. M.; White, A. B.; Hudman, R. C.; Bertschi, I. T.; Stohl, A. Chemical characteristics of North American surface layer outflow: Insights from Chebogue Point, Nova Scotia. *J. Geophys. Res.* **2006**, *111*, D23S53, doi: 10.1029/2006JD007287.
- (27) Parrish, D. D. Critical evaluation of US on-road vehicle emission inventories. *Atmos. Environ.* **2006**, *40*, 2288–2300.
- (28) Warneke, C.; de Gouw, J. A.; Stohl, A.; Cooper, O. R.; Goldan, P. D.; Kuster, W. C.; Holloway, J. S.; Williams, E. J.; Lerner, B. M.; McKeen, S. A.; Trainer, M.; Fehsenfeld, F. C.; Atlas, E. L.; Donnelly, S. G.; Stroud, V.; Lueb, A.; Kato, S. Biomass burning and anthropogenic sources of CO over New England in the summer 2004. *J. Geophys. Res.* **2006**, *111*, D23S15, doi: 10.1029/2005JD006878.
- (29) Kuhns, H.; Knipping, E. M.; Vukovich, J. M. Development of a United States–Mexico emissions inventory for the Big Bend Regional Aerosol and Visibility Observational (BRAVO) Study. *J. Air Waste Manage. Assoc.* **2005**, *55*, 677–692.
- (30) Bey, I.; Jacob, D. J.; Yantosca, R. M.; Logan, J. A.; Field, B. D.; Fiore, A. M.; Li, Q. B.; Liu, H. G. Y.; Mickley, L. J.; Schultz, M. G. Global modeling of tropospheric chemistry with assimilated meteorology: Model description and evaluation. *J. Geophys. Res.* **2001**, *106*, 23073–23095.
- (31) Wang, Y. H.; Jacob, D. J.; Logan, J. A. Global simulation of tropospheric O<sub>3</sub>-NO<sub>x</sub>-hydrocarbon chemistry: 1. Model formulation. *J. Geophys. Res.* **1998**, *103*, 10713–10725.
- (32) Hirsch, R. M.; Gilroy, E. J. Methods of fitting a straight line to data: Examples in water resources. *Water Res. Bull.* **1984**, *20*, 705–711.
- (33) Yokelson, R. J.; Urbanski, S. P.; Atlas, E. L.; Toohey, D. W.; Alvarado, E. C.; Crounse, J. D.; Wennberg, P. O.; Fisher, M. E.; Wold, C. E.; Campos, T. L.; Adachi, K.; Buseck, P. R.; Hao, W. M. Emissions from forest fires near Mexico City. *Atmos. Chem. Phys.* **2007**, *7*, 5569–5584.
- (34) Xiao, Y. P.; Jacob, D. J.; Turquety, S. Atmospheric acetylene and its relationship with CO as an indicator of air mass age. *J. Geophys. Res.* **2007**, *112*, D12305, doi: 10.1029/2006JD008268.
- (35) SMA El Inventario de Emisiones de Contaminantes Criterio de la Zona Metropolitana del Valle de México 2006. <http://www.sma.df.gob.mx/sma/>.
- (36) Barnes, D. H.; Wofsy, S. C.; Fehlau, B. P.; Gottlieb, E. W.; Elkins, J. W.; Dutton, G. S.; Montzka, S. A. Urban/industrial pollution for the New York City - Washington, DC, corridor, 1996–1998: 2. A study of the efficacy of the Montreal Protocol and other regulatory measures. *J. Geophys. Res.* **2003**, *108*, 4186, doi: 10.1029/2001JD001117.
- (37) Prinn, R. G.; Huang, J.; Weiss, R. F.; Cunnold, D. M.; Fraser, P. J.; Simmonds, P. G.; McCulloch, A.; Harth, C.; Salameh, P.; O'Doherty, S.; Wang, R. H. J.; Porter, L.; Miller, B. R. Evidence for substantial variations of atmospheric hydroxyl radicals in the past two decades. *Science* **2001**, *292*, 1882–1888.
- (38) Wang, J. S.; McElroy, M. B.; Logan, J. A.; Palmer, P. I.; Chameides, W. L.; Wang, Y.; Megretskaia, I. A. A quantitative assessment of uncertainties affecting estimates of global mean OH derived from methyl chloroform observations. *J. Geophys. Res.* **2008**, *113*, D12302, doi: 10.1029/2007JD008496.
- (39) Hurst, D. F.; Lin, J. C.; Romashkin, P. A.; Daube, B. C.; Gerbig, C.; Matross, D. M.; Wofsy, S. C.; Hall, B. D.; Elkins, J. W. Continuing global significance of emissions of Montreal Protocol-restricted halocarbons in the United States and Canada. *J. Geophys. Res.* **2006**, *111*, D15302, doi: 10.1029/2005JD006785.
- (40) Li, J. L.; Cunnold, D. M.; Wang, H. J.; Weiss, R. F.; Miller, B. R.; Harth, C.; Salameh, P.; Harris, J. M. Halocarbon emissions estimated from advanced global atmospheric gases experiment measured pollution events at Trinidad Head, California. *J. Geophys. Res.* **2005**, *110*, D14308, doi: 10.1029/2004JD005739.
- (41) Millet, D. B.; Goldstein, A. H. Evidence of continuing methylchloroform emissions from the United States. *Geophys. Res. Lett.* **2004**, *31*, L17101, doi: 10.1029/2004GL020166.
- (42) Reimann, S.; Manning, A. J.; Simmonds, P. G.; Cunnold, D. M.; Wang, R. H. J.; Li, J. L.; McCulloch, A.; Prinn, R. G.; Huang, J.; Weiss, R. F.; Fraser, P. J.; O'Doherty, S.; Grealley, B. R.; Stemmler, K.; Hill, M.; Folini, D. Low European methyl chloroform emissions inferred from long-term atmospheric measurements. *Nature* **2005**, *433*, 506–508.
- (43) EPA *Inventory of U.S. Greenhouse Gas Emissions and Sinks: 1990–2006*, Report EPA 430-R-08–005; U.S. EPA: Washington, DC, 2008.
- (44) Daniel, J. S.; Velders, G. J. M. Chapter 8: Halocarbon scenarios, ozone depletion potentials, and global warming potentials. In *Scientific Assessment of Ozone Depletion: 2006*, Global Ozone Research and Monitoring Project—Report No. 50; WMO: Geneva, 2006.
- (45) EPA *2002 National Emissions Inventory (v. 3)*; U.S. EPA: Washington, DC, 2007.
- (46) EPA *Global Anthropogenic Non-CO<sub>2</sub> Greenhouse Gas Emissions: 1990–2020*, Report EPA-430-R-06–003; U.S. EPA: Washington, DC, 2006.
- (47) Marland, G.; Boden, T. A.; Andres, R. J., Global, regional, and national CO<sub>2</sub> emissions. In *Trends: A Compendium of Data on Global Change*, Carbon Dioxide Information Analysis Center, Oak Ridge National Laboratory, U.S. DOE: Oak Ridge, TN, 2007.

ES802146J